The Canadian Mineralogist
Vol. 34, pp. 201-219 (1996)

MINERALOGY AND GEOCHEMISTRY OF FENITIZED ALKALINE ULTRABASIC SILLS OF THE GIFFORD CREEK COMPLEX, GASCOYNE PROVINCE, WESTERN AUSTRALIA

JOANNA M. PEARSON

Key Centre for Mineral Deposits, University of Western Australia, Nedlands 6907, Australia

WAYNE R. TAYLOR

Research School of Earth Sciences, Australian National University, Canberra, ACT 0200, Australia

Abstract

The Proterozoic Gifford Creek complex in Western Australia is a high-level alkaline complex hosted in ~1.8 Ga granitic basement. Magmatism occurred in two episodes. During the first phase at ~1.68 Ga, with which this paper is concerned, a swarm of ultrabasic sills (Lyons River sills) was emplaced. This was accompanied by the development of an extensive belt of fenite comparable in extent to that surrounding a major alkaline intrusive complex. However, no large bodies of alkaline rock are known from the area, suggesting that the source of fluids is an unexposed alkaline intrusive body. The later episode of magmatism at ~1.25 Ga was carbonatitic in character. Among the Lyons River minor intrusive bodies, two forms are recognized: a swarm of ultrabasic sills in which primary igneous textures are preserved, and a series of intensely deformed ultrabasic lenses. The degree of metasomatism in the fenite belt varies from pervasive K-feldspathization of the country rock in the outermost part of the aureole to intense growth of alkali amphibole and aegirine in the innermost aureole. Primary minerals in the ultrabasic sills have been replaced by alkali amphibole and aegirine, but based on the interpretation of pseudomorphs, the sills originally consisted of olivine macrocrysts set within a groundmass of mica, perovskite, titanian magnetite, and carbonate. The preserved igneous textures, *e.g.*, cm-scale layering and gravity settling of macrocrysts, are similar to those described from the Benfontein kimberlite sills in South Africa. The deformed ultrabasic lenses have been emplaced plastically, at subsolidus temperatures, into overlying sediments, possibly in response to movement on a fault. No primary textures remain, and the rock is now comprised of deformed phlogopite and potassian magnesio-arfvedsonite set in a carbonate matrix. Major- and trace-element geochemistry of the Lyons River sills shows strong affinities to carbonate-rich ultrabasic rocks such as the Benfontein sills, Igwisi Hills lavas or some examples of aillikite. Stable isotope compositions of matrix carbonates are remarkably similar to those of the Benfontein sills: $\delta^{13}C \approx -5.5‰$, $\delta^{18}O \approx +10‰$, indicating little disturbance during alkali metasomatism. Coexisting carbonates preserve compositions indicative of temperatures of fenitization above 450°C.

Keywords: alkali metasomatism, fenite, riebeckite, arfvedsonite, apatite, kimberlite, rare-earth element, cathodoluminescence, fluorine, Benfontein sills, Gascoyne Province, Western Australia.

Sommaire

Le complexe alcalin protérozoïque de Gifford Creek, en Australie occidentale, a été mis en place en deux épisodes dans un socle granitique d'environ 1.8 milliard d'années. Une venue initiale, il y a environ 1.68 Ga, a produit la suite de filons-couches ultrabasiques dite de Lyons River, et un cortège imposant de fénites, tout à fait comparable en étendue aux manifestations attendues d'un complexe intrusif alcalin majeur. Toutefois, il n'y a aucun massif volumineux dans la région, ce qui nous mène à proposer qu'un tel complexe, demeuré enfoui, a assuré la mobilisation des fluides nécessaire à la fénitisation. Le deuxième épisode de magmatisme, à environ 1.3 Ga, avait un caractère carbonatitique. Parmi les filons-couches ultrabasiques, nous reconnaissons une variété dans laquelle les textures ignées sont conservées, et une autre où nous ne trouvons que des lentilles déformées. Le degré de métasomatose atteint dans la ceinture fénitisée est variable, et mène d'une part à une feldspathisation potassique poussée des roches encaissantes dans les parties les plus distales, et d'autre part à une formation massive d'amphibole alcaline ou d'aegyrine dans les parties proximales de la ceinture. Les minéraux primaires des filons-couches ultrabasiques, dont des macrocristaux d'olivine dans une pâte à mica, pérovskite, magnétite titanifère et carbonate, ont été remplacés par une amphibole alcaline et l'aegyrine. Les textures primaires préservées, par exemple un litage centimétrique et une accumulation des macrocristaux par gravité, ressemblent à celles qui ont été décrites dans les filons-couches kimberlitiques de Benfontein, en Afrique du Sud. Les lentilles déformées témoignent d'un remaniement plastique, à une température sous le solidus, dans une séquence de roches sédimentaires sus-jacentes, peut-être suite au mouvement le long d'une faille. Il ne reste rien des textures primaires dans ces lentilles; la roche contient maintenant phlogopite et magnésio-arfvedsonite potassique déformées dans une pâte carbonatée. D'après leur filiation géochimique (éléments majeurs et traces), les filons-couches de Lyons River ressemblent beaucoup aux roches ultrabasiques riches en carbonate, telles que documentées dans les filons-couches de Benfontein, les laves de Igwisi Hills, et certains exemples d'aillikite. Les rapports d'isotopes stables des carbonates de la pâte, en particulier, se rapprochent remarquablement des valeurs décrites pour Benfontein: $\delta^{13}C \approx -5.5‰$, $\delta^{18}O \approx +10‰$. Ces rapports n'auraient donc pas été sensiblement modifiés au cours de la métasomatose alcaline. La composition des carbonates coexistants indique une température de fénitisation supérieure à 450°C.

(Traduit par la Rédaction)

Mots-clés: métasomatose alcaline, fénite, riebeckite, arfvedsonite, apatite, kimberlite, terres rares, cathodoluminescence, fluor, filons-couches de Benfontein, province de Gascoyne, Australie occidentale.

INTRODUCTION

The Gascoyne Province comprises high-grade metamorphic and granitic basement rocks of the Paleoproterozoic Capricorn Orogen, located between the Archean Pilbara and Yilgarn Cratons in Western Australia (Williams 1986, Fig. 1). The Province is overlain to the east by Mesoproterozoic sedimentary rocks of the Bangemall Basin (Chuck 1984, Muhling & Brakel 1985). Alkaline rocks have not previously been described from this area, although rare-earth-element-bearing "ironstones" (known informally as the Yangibana ironstones) of assumed carbonatitic affinity, were recognized by various mining companies (Gellatly 1975, Newcrest Mining Ltd. 1989). Recent mapping (1992–1994) by the present authors indicates that the ironstones are one of a number of high-level alkaline intrusive bodies. They are exposed in a ~700 km^2 area that includes extensive zones of fenitized rock. These exposures collectively make up a newly recognized alkaline complex informally termed the Gifford Creek complex (GCC). The fenites of the GCC comprise the largest area of alkali metasomatic rocks presently recognized in Australia.

Detailed field mapping of the GCC has established various types of minor intrusive bodies based on style of emplacement and mineralogical composition. In this paper, we are mainly concerned with alkali amphibole- and sodic pyroxene-rich ultrabasic sills (the "Lyons River sills"), and associated deformed lenses. They form a swarm parallel to the Lyons River valley and are associated with an extensive belt of country-rock fenitization (Figs. 2a, 3). Other minor intrusive bodies include the Yangibana ironstones,

FIG. 2. a) Simplified geological map of the Gifford Creek complex. b) Enlarged map of the Radfords Rise location, showing detail of deformed ultrabasic lens.

→

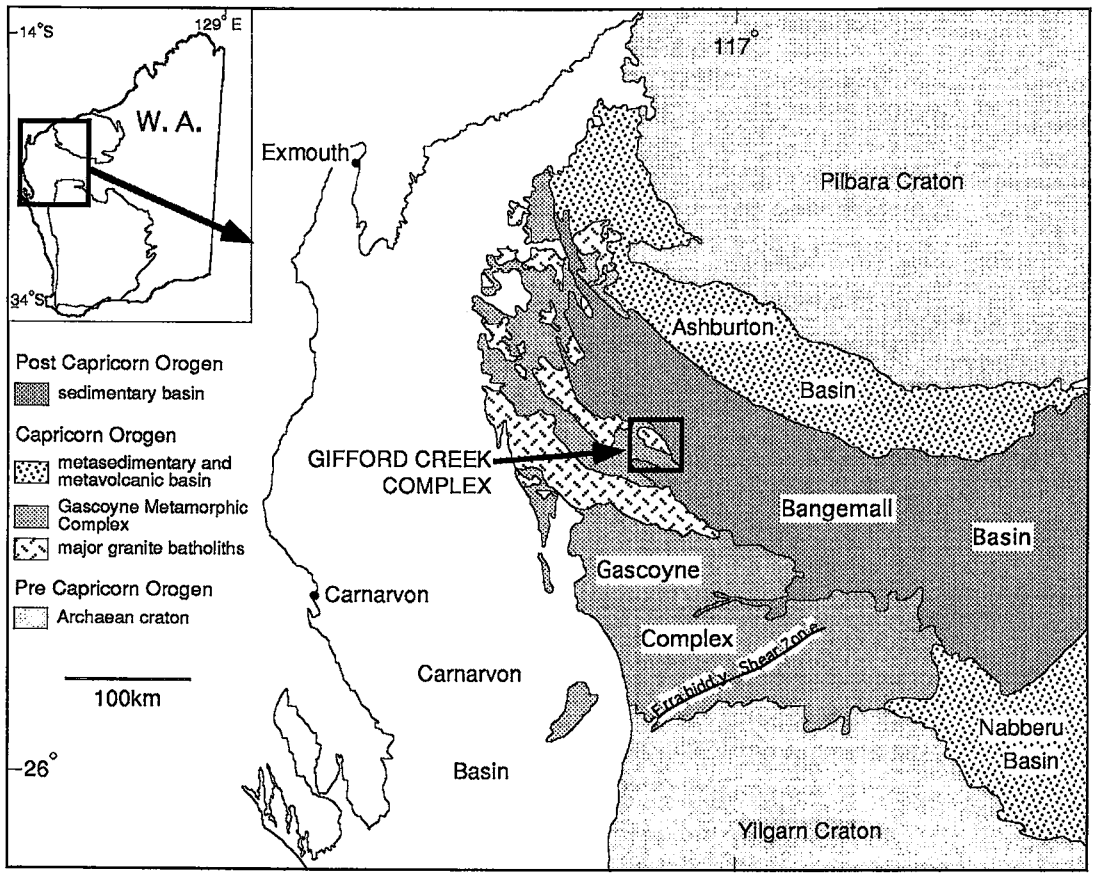

FIG. 1. Geological map of the Capricorn Orogen, showing location of the Gifford Creek complex.

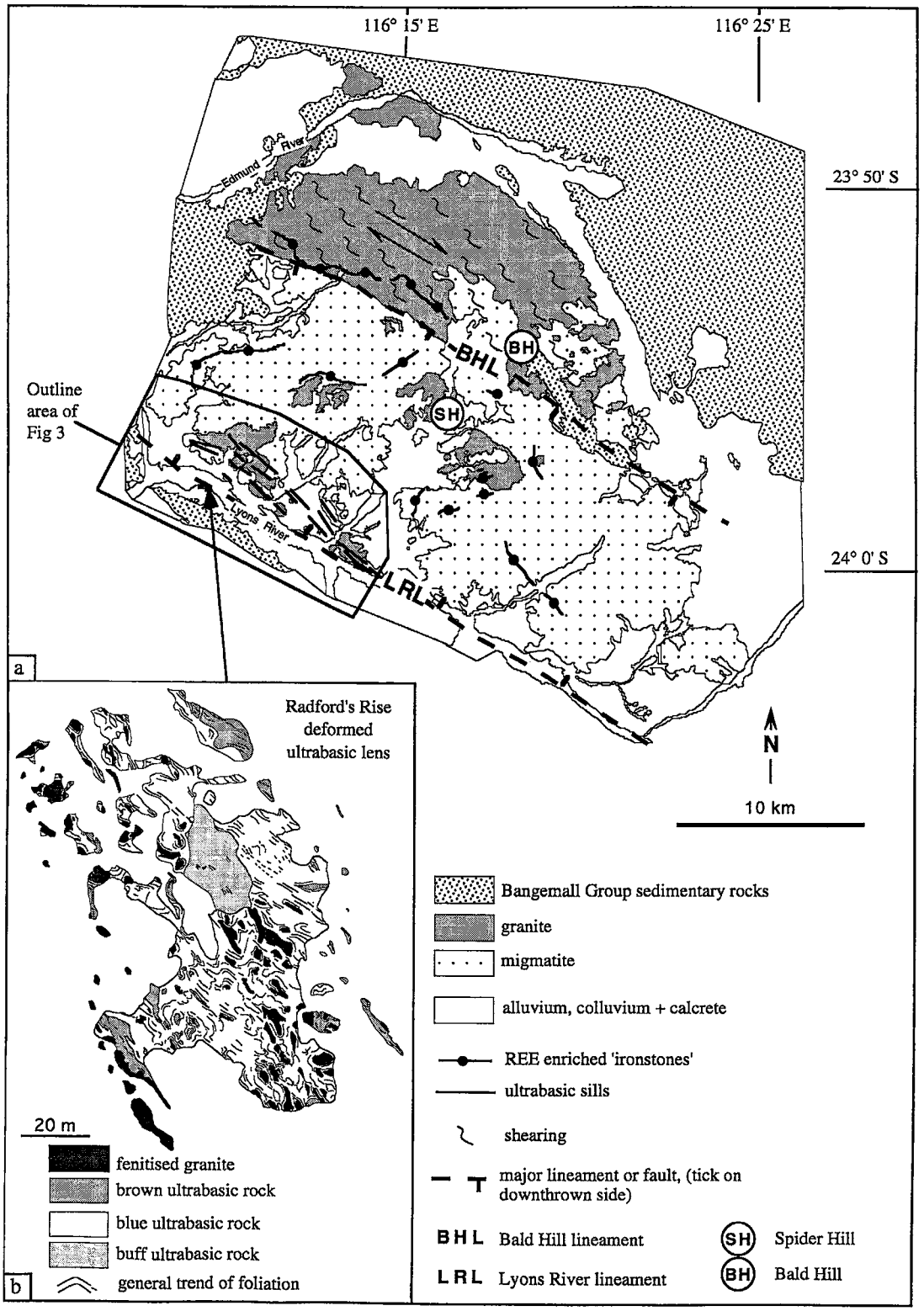
116° 15' E
116° 25' E
23° 50' S
24° 0' S
Edmund River
Lyons River
BHL
LRL
BH
SH
Outline area of Fig 3
a
N
10 km
Radford's Rise deformed ultrabasic lens
20 m
fenitised granite
brown ultrabasic rock
blue ultrabasic rock
buff ultrabasic rock
general trend of foliation
b
Bangemall Group sedimentary rocks
granite
migmatite
alluvium, colluvium + calcrete
REE enriched 'ironstones'
ultrabasic sills
shearing
major lineament or fault, (tick on downthrown side)
BHL Bald Hill lineament
LRL Lyons River lineament
SH Spider Hill
BH Bald Hill

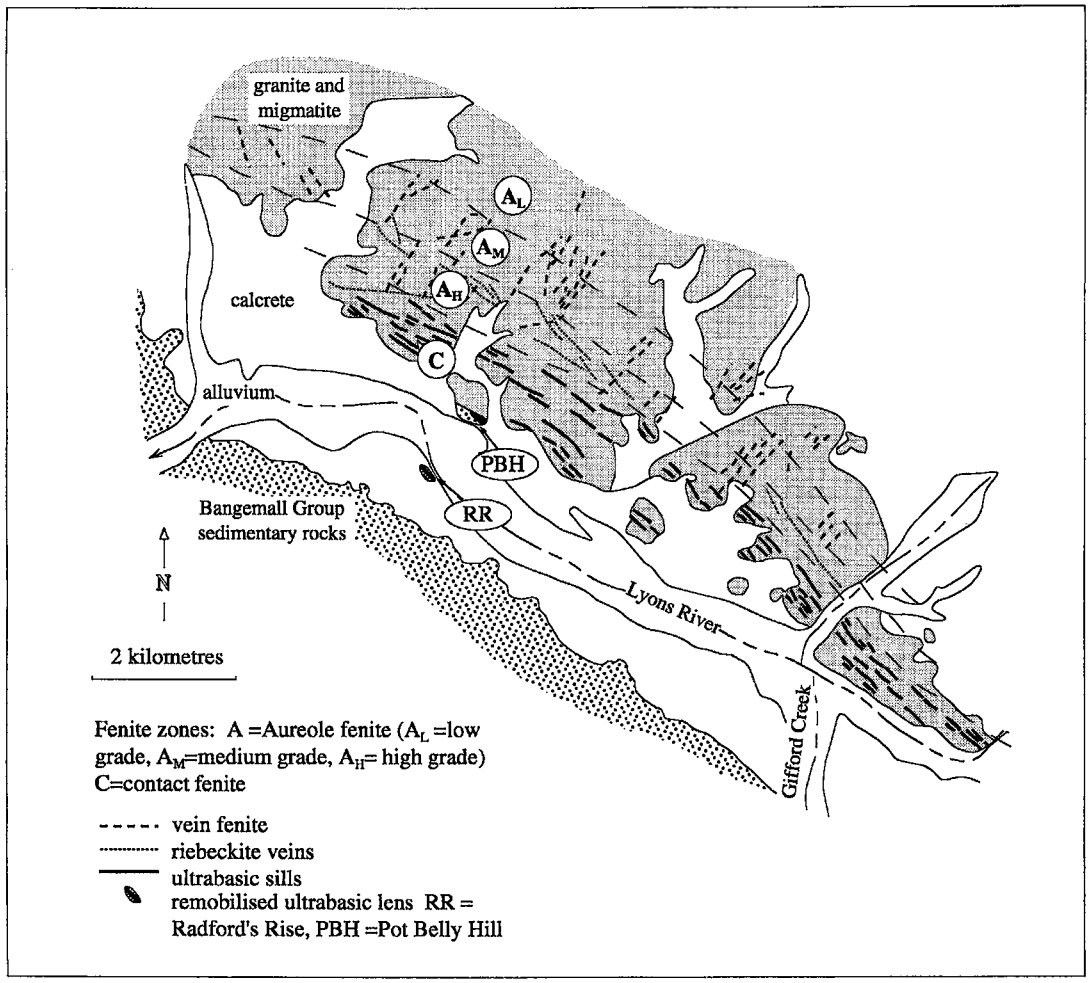

FIG. 3. Sketch map of fenite zones associated with the Lyons River ultrabasic sills and lenses.

which are magnetite- and hematite-rich pods (~40 to 150 m^2) having marked radioactivity. The pods are enclosed by sinuous zones of K-feldspar – magnetite alteration and are traceable to narrow ferrocarbonatite dykes at depth (Gellatly 1975, Newcrest Mining Ltd. 1989). Narrow flat-lying aegirine – apatite – phlogopite – magnetite – pyrochlore-bearing sheets occur in the center of the complex (Spider Hill, Fig. 2a) and are gradational into the magnetite pods. Limonitic, weathered intrusive rocks occur within basal layers of an inlier of Bangemall Group sedimentary rocks (Bald Hill, Fig. 2a) and rare fluidization breccias are exposed in the basement granitoid rocks.

Preliminary SHRIMP dates determined on zircon separates indicate that the Lyons River sills and the magnetite-rich (ferrocarbonatitic) intrusive bodies were emplaced at approximately 1.68 Ga and 1.25 Ga, respectively (J. Pearson, unpubl. results). Field relationships suggest that the emplacement of the Lyons River sills and the development of the associated belt of fenitized rock occurred prior to Bangemall Group sedimentation, and the remaining intrusive bodies, and deformation of the sills, occurred after initiation of Bangemall sedimentation.

Our aim in this paper is to document the texture, mineralogy, nature of metasomatism, and geochemistry of the Lyons River ultrabasic sills and deformed lenses, and to compare the Lyons River sills with apparently similar intrusive bodies from Benfontein, South Africa. Such rocks have not previously been documented from any Australian locality.

Methods

Identification of alteration and metasomatic minerals was undertaken with standard petrographic techniques and by X-ray powder diffractometry of mineral separates. Cathodoluminescence (CL) photomicrographs and observations were undertaken on polished thin sections and rock slabs using a Nuclide luminoscope at University College London, operating at ~0.8 mA and ~12 kV accelerating voltage. Room temperature CL spectra of zoned apatite grains were recorded over the range 400 to 700 nm with an Oxford Instruments monoCL grating spectrometer attached to a JEOL 6400 SEM at Oxford Instruments Research Laboratories, Eynsham, England. To avoid beam damage to the specimen, the spectra were obtained at 10 kV by signal averaging the output of several 20 μm by 20 μm areas.

Mineral compositions were determined by wavelength-dispersion analysis (WDS) using a fully automated CAMECA SX50 electron-probe microanalyzer at the Natural History Museum, London, operated at an accelerating voltage of 20 kV and a beam current of 20 nA, and calibrated with a range of synthetic and natural standards. Additional analyses were performed by energy-dispersion spectrometry (EDS) using a LINK PC–XA system on a JEOL 6400 SEM. Reduction of the EDS data followed the method of Ware (1980).

Concentrations of major elements and Nb, Zn, V, Zr, Y, Sr, Ba, Rb, U, Cr, As, Pb, Mo and W, obtained on pressed powder pellets, were determined by X-ray fluorescence (XRF) spectrometry at Analabs Analytical Laboratories, Perth. Concentrations of rare-earth elements, and of Hf, Sc, Ta and Th, were determined by instrumental neutron activation (INAA) at Becquerel Laboratories, Lucas Heights, Sydney. The concentration of fluorine was determined by NaOH fusion-specific ion electrode analysis at Acme Laboratories Ltd, Vancouver, with an accuracy of ±10% or better. In all cases, analytical accuracy was confirmed against various international reference materials and internal standards. XRF determinations are accurate to ±2% for the major elements and to better than ±10% for the traces. INAA determinations are accurate to better than ±5% for the light rare-earth elements (*LREE*) (La to Eu) and to better than ±15% for the remaining elements.

Carbon and oxygen isotope compositions were determined on carbonate mineral separates (magnesite and dolomite) from two samples of the Lyons River ultrabasic sills by phosphoric acid CO_2 extraction using procedures and corrections outlined by Golding *et al.* (1987). Analytical uncertainties are up to ±0.5‰ for carbonate oxygen because of possible errors in estimation of the acid fractionation factor of the dominant carbonate.

Metasomatic Zonation

The ultrabasic sills and lenses are associated with a belt of alkali-metasomatic alteration (fenitization) of the country-rock granites and migmatites parallel to the Lyons River (Fig. 3). The metasomatic belt is asymmetrical from north to south, and about 5 km in width. The most intensely fenitized zone lies mostly under recent cover along the Lyons River. Following the fenite classification scheme of Kresten (1988), three styles of fenite alteration are recognized:

Aureole fenites of ~2–4 km width occupy most of the belt. Furthest from the Lyons River, in the lowest-grade part of the aureole, the country-rock granitoid rocks show pervasive sericitization of plagioclase and incipient growth of K-feldspar, but primary textures are generally well preserved. Closer to the Lyons River, the granitoid rocks show progressive replacement of biotite, quartz and plagioclase by K-feldspar, sericite and alkali amphibole (medium- to high-grade aureole fenites). The K-feldspar is too fine-grained to optically determine the structural state. Small stocks of "syenite", presumably arising from extreme, but localized, K-feldspathization of the country rocks, are developed in the high-grade aureole.

Vein fenites cross-cut the aureole fenites and vary from K-feldspar-rich veins in the medium-grade part of the aureole to alkali-amphibole-rich veins in the higher-grade parts. The alkali amphibole veins may be discontinuous and contain "clots" of riebeckite, together with angular clasts of the feldspathized country-rock. The coarse-grained K-feldspar in these veins is turbid, with a patchy pattern, and is devoid of grid twinning, but is similar in appearance to the description of microcline from other fenitic assemblages (Siemiatkowska & Martin 1975).

The *contact fenite* zone contains the ultrabasic sills and deformed lenses. Fenitization of the host granitoid rocks is extreme, with near-complete replacement of the original minerals by K-feldspar, alkali amphibole, sodic pyroxene and carbonate. Only trace amounts of quartz, mica, or plagioclase remain. The primary mafic minerals of the ultrabasic sills and deformed lenses have been completely replaced by alkali amphibole and sodic pyroxene.

Lyons River Ultrabasic Sills and Deformed Lenses

The ultrabasic intrusive bodies comprise a swarm of sills showing relatively undeformed primary igneous textures. They are ~0.5–2 m in width and are traceable in length for many tens of meters. The ultrabasic sills are confined to the basement and cross-cut the rock fabric of the host granitoid rocks as well as earlier K-feldspar metasomatic veins. The deformed lenses, on the other hand, occur as bulbous pods within undeformed porphyritic granite and as narrow lenses

along the basal unconformity with sedimentary rocks of the Bangemall Group. The two types of intrusive bodies are distinctly different and will be described separately.

Primary-textured ultrabasic sills

Although the ultrabasic rocks have been metasomatized and the primary minerals have been almost completely replaced, the textures are preserved, with very little deformation. The textures are best explained in igneous petrographic terms. The original minerals can be identified in most cases, although the replacing mineral phase varies with sill type. The sills can be grouped into four main textural–mineralogical types:

Blue sills are the most common type. In hand specimen, the rock has a distinctive blue color and is generally porphyritic, with ~2 mm macrocrysts set in a fine-grained, carbonate-rich matrix. The pseudomorphs may have eudedral outlines, or occur as more rounded "blebs" consisting of a fine-grained mat of alkali amphibole and carbonate. They are set in a mosaic of fine-grained carbonate together with either coarser-grained blue amphibole or sodic pyroxene needles, and fine-grained apatite, barite, monazite, zircon, phlogopite, and a trace of K-feldspar. Cathodoluminescence studies reveal that apatite may make up to ~5–10% of the rock. Rutile intergrown with carbonate has replaced abundant ~0.25 mm grains and smaller ~0.1 mm grains of cubic shape; some of these were originally twinned or intergrown crystals. These features suggest that the original minerals were probably perovskite and titanian magnetite. Other minerals include fine irregular Fe-oxides and rare grains of pyrite. Less common minerals are rare ~1 mm phenocrysts of zoned mica replaced by secondary phases, and ~1 mm lath-shaped phenocrysts, now a mosaic of K-feldspar and carbonate, possibly after primary carbonate or mica.

The blue sills commonly contain crystal-rich zones suggestive of gravity settling of macrocrysts, and fine centimeter-scale layering reminiscent of multiple-magma-injection textures in the Benfontein sills (Dawson & Hawthorne 1973). Other intrusive bodies are composite sills with ~10 to 50-cm thick layers in which carbonate-rich layers are overlain by macrocryst-rich layers. Sedimentary-style load structures and a high concentration of Fe–Ti-oxides may be observed along the interface between the layers (Fig. 4a).

Light brown sills are less common. In hand specimen, the rock is generally porphyritic in appearance; however, the 1–2 mm phenocrysts weather out, leaving cavities similar to those found on weathered ultramafic rocks. The phenocrysts, which are mostly of prismatic form and reminiscent of olivine and clinopyroxene, may be concentrated in layers, again suggestive of gravity settling. The phenocrysts, which are replaced by carbonate, are set in a fine-grained mosaic of carbonate, sodic pyroxene needles, abundant apatite and barite. Opaque oxides are less abundant than in the blue sills (Fig. 4b).

Dark brown sills are rare. They weather to a fine-grained, Fe-oxide-rich, brown porphyritic rock, with abundant glistening ~0.5 mm phenocrysts of mica and rounded ~2 mm macrocrysts now replaced by carbonate and Fe-oxides (hematite and goethite). The matrix minerals comprise largely fine-grained carbonates and Fe-oxide, with lesser fine-grained matrix mica that also mantles the mica phenocrysts (Fig. 4c).

Green sills are fine grained and equigranular. Macrocrysts are notably absent. Green sills are carbonate-rich (>60% carbonate), and consist of a fine equigranular mosaic of carbonate, with abundant fine-grained apatite, and radiating needles of sodic pyroxene (Fig. 4d).

In all the types of sill, sodic pyroxene is not observed to replace olivine, and where olivine has been replaced by carbonate only, the groundmass invariably contains sodic pyroxene rather than alkali amphibole. Alkali amphibole and sodic pyroxene do not occur together in the groundmass, and where sodic pyroxene is dominant in the groundmass, apatite is more abundant.

Field evidence has not established the relative timing of the blue, light brown and dark brown sills, as they are subparallel, and cross-cutting relations have not been observed. However, the green sills are late as they cross-cut the blue sills.

Deformed lenses

The deformed lenses are composed predominantly of carbonate, alkali amphibole and phlogopite, with lesser amounts of apatite, rutile, monazite, barite, and rare zircon. They are strongly deformed, without relics of their primary igneous texture. Where the lenses have been emplaced into the basal Bangemall unconformity, as at the Pot Belly Hill locality (Fig. 2), the host sedimentary rocks have become deformed in a style resembling soft-sediment folding, and intermixed within the margins of the body. This suggests that the Bangemall sedimentary rocks were largely unconsolidated at the time of emplacement. The emplacement appears to have occurred after the fenitization event and at relatively low temperatures, as there is no evidence for contact metamorphism or for fenitization of the sedimentary rocks; neither is there textural evidence for explosive volcanic activity, as would be the case if the bodies were emplaced as a diatreme, for example.

Some lenses exhibit multiple phases of intrusion, which can be distinguished primarily on the color of the weathered outcrop. At the Radfords Rise locality (Fig. 2b), the earliest phase, occurring on the margins of the lenses, is a brown-colored rock. It is composed

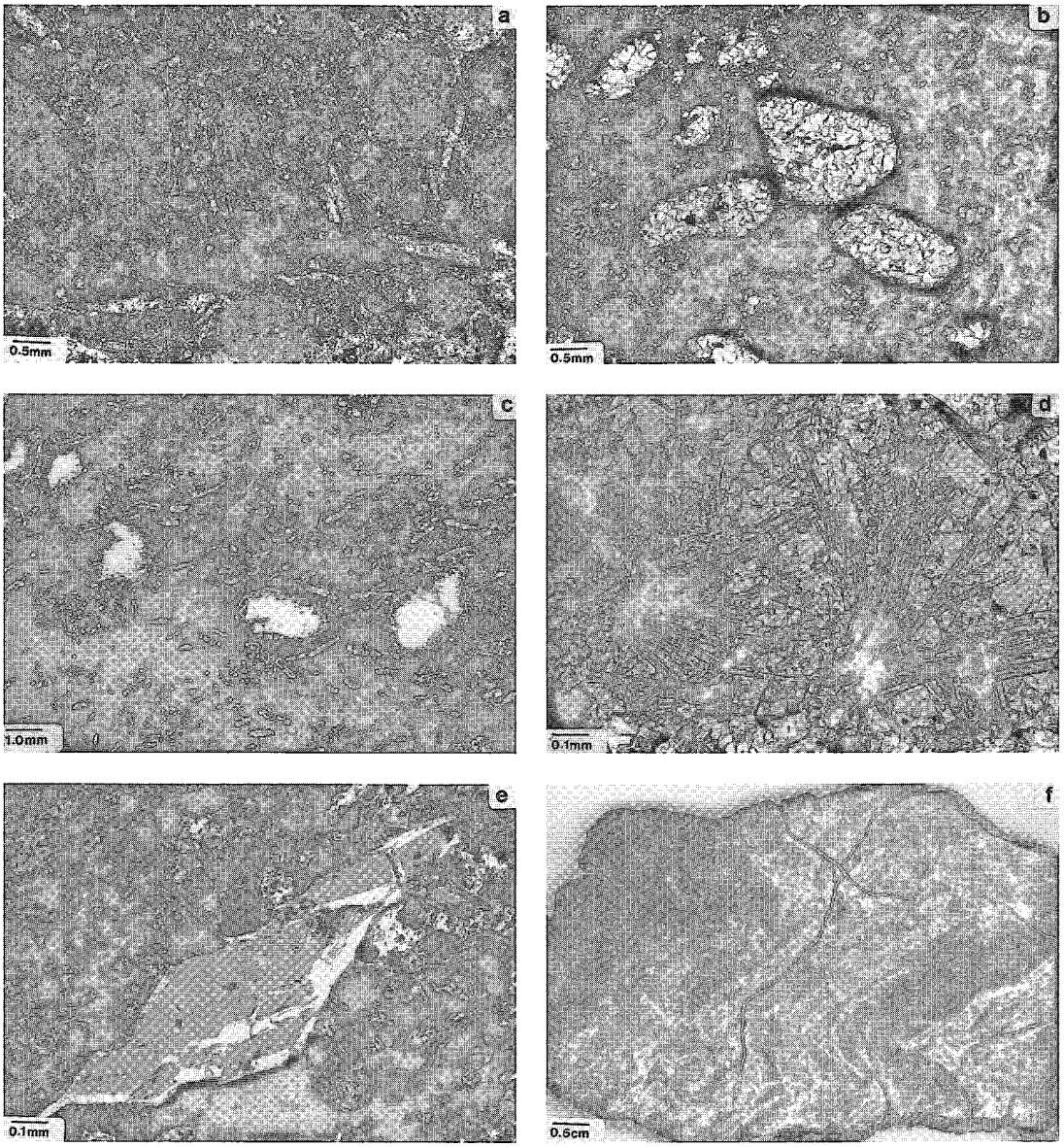

FIG. 4. Photomicrographs of representative samples of Lyons River sills and deformed lenses. a) Blue sill, showing replaced olivine macrocrysts and lath-shaped minerals, possibly after carbonate, in a finer groundmass of rutile pseudomorphs after perovskite and carbonate. Fine needles of aegirine also present in the groundmass cannot be discerned on the photograph. b) Light brown sill, showing phenocryst phase replaced by a fine-grained mosaic of carbonate, set within a matrix of carbonate, apatite, and aegirine. c) Dark brown sill, showing indistinct macrocrysts after olivine, and mica phenocrysts, in a groundmass of fine-grained carbonate, Fe-oxides, and fine-grained phlogopite. d) Green sill, showing radiating needles of aegirine within an aphanitic carbonate groundmass. e) Deformed lens, showing brittly deformed K-Mg-arfvedsonite crystals set in a carbonate-rich groundmass. f) Deformed lens. Photograph of polished rock surface, showing the intense plastic deformation that is characteristic of this rock type.

primarily of carbonate, phlogopite, and ilmenite, with "trails" of fine-grained blue amphibole, and contains ~1–2 cm angular clasts of very fine-grained massive phlogopite. The lens is brecciated and redistributed by a blue-colored lens. Within the blue phase, there are poorly defined ~0.5–2 m long lenses of sodic-

pyroxene-rich rock in which the pyroxene forms coarse-grained "knots" within a sodic pyroxene – carbonate matrix. The blue lens contains distinctive ~0.5 mm crystals of alkali amphibole and grains of mica that are attenuated and broken, and in some cases rotated (Fig. 4e). They are set in a matrix composed of a fine-grained, equigranular carbonate that shows evidence of plastic flow (Fig. 4f). In the center of the outcrop is an apparently late, poorly exposed, buff-colored lens in which clasts of country rock or earlier intrusive phases are absent.

Late veins

At the Radford's Rise deformed lens locality, late veins consisting of coarse-grained alkali amphibole, rhombs of dolomite and coarse-grained masses of ilmenite, in some cases >30 cm in size, cross-cut the body. Elsewhere, ~1-cm-wide veins, containing coarse-grained dolomite and apatite, cross-cut the ultrabasic sills. Late quartz – Fe-oxide veins with feldspathized envelopes cross-cut and locally disrupt the ultrabasic sills.

Mineral Chemistry

Alkali amphibole

Alkali amphibole has been analyzed from the ultrabasic sills and deformed lenses, and from incorporated clasts of fenitized granite. The amphiboles vary in composition from potassian magnesio-arfvedsonite to magnesio-riebeckite (IMA classification). Representative compositions are given in Table 1. Because the amphiboles contain only minor amounts of Al, the proportion of ferric ion in the amphiboles was calculated from the microprobe analyses by setting Si to 8 cations, following the scheme of Hawthorne (1981). This procedure yields, in most cases, a valid crystal-chemical solution such that for 23 atoms of oxygen, cation totals fall between 15 and 16, and the *M*1–3 and *M*4 sites are full or have minor vacancies (≤3%). Cation-site vacancies of this order in alkali amphiboles are a phenomenon that was noted by Hawthorne (1976). In some alkali amphibole compositions, normalization of Si to 8 cations creates a crystal-chemically unacceptable solution (total cations >16); for these compositions, the proportion of ferric ion was estimated by normalizing total cations to 16 (Hawthorne 1981).

Compositional variation of the alkali amphiboles is shown in Figures 5a and 5b. Amphiboles in the ultrabasic sills show strong compositional zonation in both mg# and Na/(Na+K) ratio, whereas amphibole zonation in the remobilized lenses is weak and involves only slight decrease in mg# (Table 1). There is no noticeable difference in composition between the amphiboles in the replaced macrocrysts and in the groundmass. Amphibole cores in the ultrabasic sills, and amphibole grains in the remobilized lenses and fenite clasts, are rich in the $KNa_2Mg_4Fe^{3+}Si_8O_{22}F_2$ (potassian magnesio-fluor-arfvedsonite) component. Amphibole rims and unzoned grains in the sills grade toward magnesio-riebeckite-rich compositions that are poor in K and F (Fig. 5b). Two amphibole compositions have extreme K contents (~7.5 wt% K_2O) that appear from a literature search to be significantly higher than previously reported values for arfvedsonite (For instance, Mian & Le Bas (1986) reported up to 3.27 wt% K_2O in magnesio-arfvedsonite from the Loe Shilman carbonatites). Conventional schemes of cation allocation to the *T*, *M*1–3, *M*4 and *A* sites are not applicable for these arfvedsonitic compositions. Specifically, Fe^{3+} is required in the *T* site, K is required in the *M*4 site, and Ca and a small amount of Na must be allocated to the *M*1–3 sites to achieve acceptable site totals.

TABLE 1. REPRESENTATIVE COMPOSITIONS OF ALKALI AMPHIBOLE FROM ULTRABASIC SILLS, LENSES AND FENITE

	ULTRABASIC SILLS			DEFORMED LENSES			FENITE
TYPE	blue	blue	blue				
SAMPLE	P16852	P01019	P01019	P17401	P17401	P17402	P01093
core/rim	*	c	r	c	r	*	*
wt%							
SiO_2	55.05	55.28	54.43	54.78	55.16	54.51	54.34
TiO_2	0.54	0.25	0.01	0.07	0.08	0.25	0.32
Al_2O_3	0.33	0.06	0.47	0.03	0.08	0.06	0.07
Cr_2O_3	0.05	0.09	0.08	0.12	0.14	0.03	bld
Fe_2O_3*	12.58	13.21	16.84	10.38	9.99	11.00	11.07
FeO*	7.37	1.16	5.99	3.50	4.67	3.74	4.99
MnO	bld	bld	bld	bld	bld	0.04	0.06
MgO	11.98	14.59	10.15	15.68	15.07	14.90	13.68
CaO	0.58	0.18	0.51	0.14	0.32	0.69	0.09
Na_2O	6.97	7.31	7.12	6.24	6.70	5.93	6.71
K_2O	1.76	4.50	0.13	5.36	5.24	7.60	5.05
F	0.36	2.27	0.07	1.44	1.62	1.15	1.83
O = F	0.15	0.96	0.03	0.61	0.68	0.48	0.77
Total	97.42	97.95	95.77	97.13	98.39	99.42	97.46
O = 23							
Si	8.000	8.000	8.000	8.000	8.000	7.903	8.000
$Al^{(iv)}$	0.000	0.000	0.000	0.000	0.000	0.010	0.000
Fe^{3+}	0.000	0.000	0.000	0.000	0.000	0.087	0.000
Ti	0.059	0.027	0.001	0.007	0.008	0.027	0.035
$Al^{(vi)}$	0.056	0.010	0.081	0.004	0.014	0.000	0.012
Cr	0.000	0.000	0.000	0.000	0.000	0.003	-
Fe^{3+}	1.376	1.439	1.863	1.141	1.090	1.113	1.226
Mg	2.595	3.148	2.224	3.414	3.259	3.220	3.002
Fe^{2+}	0.896	0.140	0.736	0.427	0.566	0.453	0.614
Mn	-	-	-	-	-	0.004	0.007
Ca	0.018	0.028	0.080	0.000	0.000	0.107	0.000
Na	0.000	0.051	0.015	0.000	0.000	0.073	0.000
Ca	0.072	0.000	0.000	0.022	0.049	0.000	0.013
Na	1.928	2.000	2.000	1.768	1.884	1.594	1.916
K	0.000	0.000	0.000	0.000	0.000	0.406	0.000
Na	0.035	0.000	0.014	0.000	0.000	0.000	0.000
K	0.326	0.831	0.024	0.999	0.970	1.000	0.948
Cation Total	15.366	15.674	15.038	15.797	15.858	16.000	15.770
mg #	74.3	95.7	75.1	88.9	85.2	87.7	83.0
tet	8.000	8.000	8.000	8.000	8.000	8.000	8.000
M1-3	5.000	4.843	5.000	4.993	4.937	5.000	4.896
M4	2.000	2.000	2.000	1.790	1.933	2.000	1.929
A	0.361	0.831	0.038	0.999	0.970	1.000	0.948

bld = below level of detection
nc = none calculated
c = calculated

Sodic pyroxene

The sodic pyroxene in all the rock types investigated (sills, lenses and fenites) is aegirine

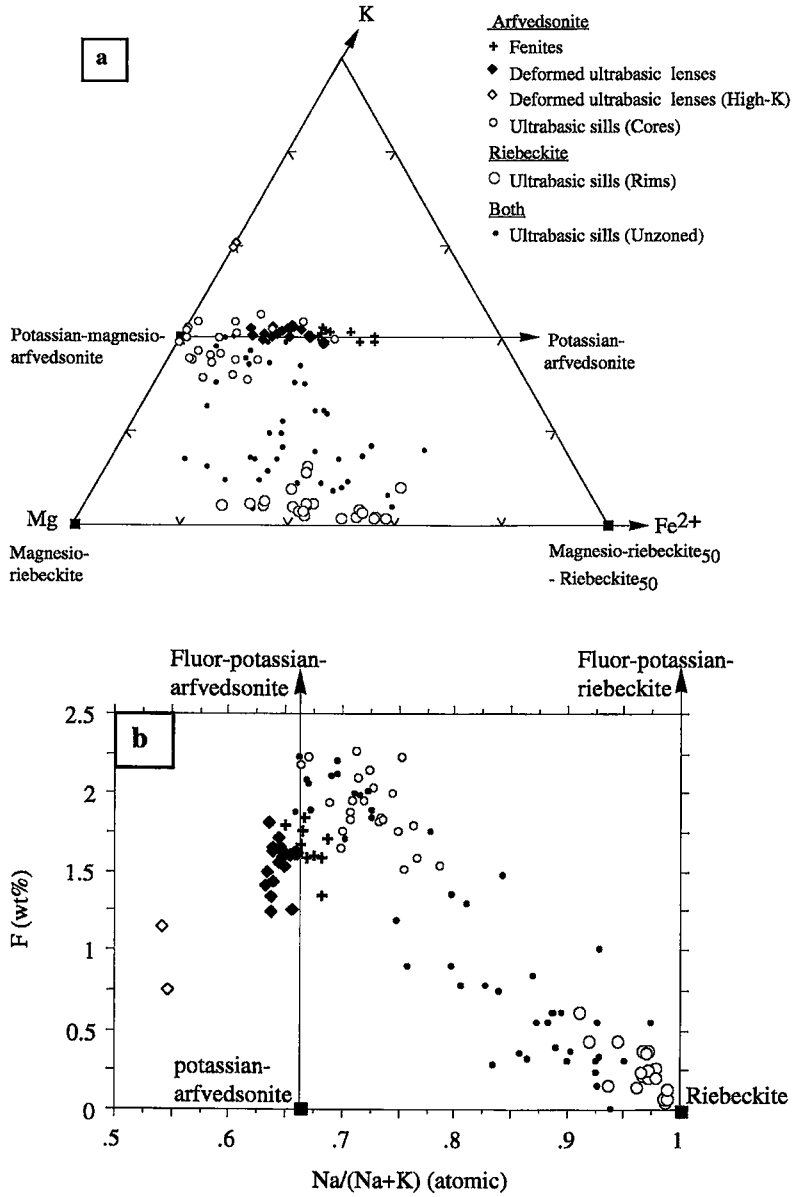

FIG. 5. Compositional variation of alkali amphibole from the Lyons River ultrabasic sills lenses and fenites plotted on a) a K–Mg–$Fe^{2+}_{(total)}$ diagram to show discrimination between potassian magnesio-arfvedsonite and magnesian riebeckite for the amphibole cores in the remobilized lenses. b) F (wt%) *versus* Na/(Na + K) (atomic) to show the decrease in F content from core of sample to rim, and the high fluorine content of the remobilized lenses.

with a high (mostly >90 mol.%) $NaFe^{3+}Si_2O_6$ component (Table 2). Ti is the only other significant minor element, with a maximum content of ~4 wt% TiO_2. There are no significant differences in composition of the sodic pyroxene among rock types.

TABLE 2. REPRESENTATIVE COMPOSITIONS OF PYROXENE FROM ULTRABASIC SILLS AND FENITE

	ULTRABASIC SILLS			FENITE			
TYPE	blue	blue	blue				
SAMPLE	76707†	76718†	76718†	P01093‡	P01093‡	P01093‡	P01093‡
wt%							
SiO_2	50.78	53.22	52.95	51.81	52.11	51.87	51.88
TiO_2	0.37	3.11	1.62	3.48	2.77	0.11	3.13
ZrO_2	na	na	na	bld	0.08	0.02	0.07
Al_2O_3	0.50	bld	0.31	0.07	0.02	0.07	0.05
Cr_2O_3	0.35	0.16	bld	0.09	0.01	0.30	0.03
V_2O_3	na	na	na	0.24	0.06	0.34	0.06
Fe_2O_3c	29.55	27.85	29.62	26.70	28.22	32.06	27.31
FeOc	4.04	3.26	2.24	2.09	1.80	0.94	2.06
MnO	0.14	bld	bld	0.02	bld	bld	0.02
MgO	bld	0.67	0.22	0.89	0.52	0.04	0.80
CaO	0.16	0.28	0.44	0.09	0.07	0.09	0.07
Na_2O	12.22	13.29	13.28	13.17	13.33	13.13	13.20
K_2O	bld	bld	bld	0.06	0.06	0.04	0.03
Total	98.11	101.84	100.68	98.73	99.07	99.02	98.71
O=6							
Si	2.001	2.000	2.013	1.999	2.007	2.012	2.003
Ti	0.011	0.088	0.046	0.101	0.080	0.003	0.091
Zr	-	-	-	-	0.001	-	0.001
Al	0.023	-	0.014	0.003	0.001	0.003	0.002
Cr	0.011	0.005	-	0.003	-	0.009	0.001
V	-	-	-	0.007	0.002	0.011	0.002
Fe3	0.876	0.788	0.847	0.775	0.818	0.936	0.794
Fe2	0.133	0.102	0.071	0.067	0.058	0.031	0.066
Mn	0.005	-	-	0.001	-	-	0.001
Mg	-	0.038	0.012	0.051	0.030	0.002	0.046
Ca	0.007	0.011	0.018	0.004	0.003	0.004	0.003
Na	0.934	0.968	0.979	0.985	0.996	0.988	0.988
K	-	-	-	0.003	0.003	0.002	0.002
Cation Total	4.000	4.000	4.000	4.000	4.000	4.000	4.000
mg #	0	26.8	14.9	43.3	33.8	6.7	40.8

† = EDS analysis
‡ = WDS analysis
na = not analysed
c = calculated
bld = below level of detection

TABLE 3. REPRESENTATIVE COMPOSITIONS OF MICA FROM ULTRABASIC SILLS AND DEFORMED LENSES

	ULTRABASIC SILLS						DEFORMED LENS
TYPE	blue	blue	blue	blue	dark-brown(p)	dark-brown(m)	
SAMPLE	76716	P01019	P01019	P16852	P17118	P17118	P01090
wt%							
SiO_2	43.74	42.96	44.31	41.64	35.49	38.92	41.59
TiO_2	0.99	0.99	0.89	1.01	5.07	1.72	1.07
Al_2O_3	9.18	9.77	9.16	10.15	13.83	13.04	8.23
V_2O_3	0.04	bld	bld	0.04	0.07	0.11	0.04
Cr_2O_3	bld	0.04	0.05	bld	0.25	0.09	0.08
Fe_2O_3tc	7.32	8.56	7.16	10.93	nc	18.60	15.05
FeOtc	nc	nc	nc	nc	17.67	nc	nc
MnO	bld	bld	bld	0.03	bld	bld	bld
MgO	21.86	21.40	21.53	20.47	13.30	14.72	18.28
CaO	bld	bld	bld	0.03	0.11	0.13	0.16
Na_2O	0.07	bld	0.06	0.04	0.06	0.08	0.25
K_2O	10.73	10.52	10.8	9.74	8.61	9.70	9.26
BaO	0.04	bld	bld	bld	0.37	0.13	0.05
F	3.89	3.81	3.99	2.00	0.64	1.04	2.97
F=O	1.64	1.6	1.68	0.84	0.27	0.44	1.25
Total	96.25	96.58	96.30	95.25	95.22	97.86	95.78
O=22							
Si	6.287	6.172	6.357	6.028	5.427	5.592	6.097
Ti	0.107	0.107	0.096	0.110	0.583	0.186	0.118
Al	1.555	1.654	1.549	1.732	2.493	2.208	1.422
Cr	-	0.005	0.006	-	0.030	0.010	0.009
V	0.005	-	-	0.005	0.009	0.013	0.005
Fe^{3+}	0.792	0.925	0.773	1.191	0.000	2.011	1.660
Fe^{2+}	0.000	0.000	0.000	0.000	2.260	0.000	0.000
Mn	-	-	-	0.004	-	-	-
Mg	4.684	4.584	4.604	4.418	3.032	3.153	3.995
Ca	-	-	-	0.005	0.018	0.020	0.025
Na	0.020	0.028	0.017	0.011	0.018	0.022	0.071
K	1.968	1.928	1.977	1.799	1.680	1.778	1.732
Ba	0.002	-	-	-	0.022	0.007	0.003
Cation Total	15.420	15.403	15.379	15.303	15.572	15.000	15.137
mg #	100.0	100.0	100.0	100.0	57.3	100.0	100.0

bld = below level of detection
t = all iron either as FeO of Fe2O3
c = calculated
(p) = phenocryst sample
(m) = mantle sample

Mica

Representative compositions of metasomatic mica from the blue and dark brown ultrabasic sills, and from the deformed lenses, together with the composition of a primary phenocrystic mica from a dark brown sill, are given in Table 3. For the purposes of comparison, Fe in the metasomatic mica has been recalculated as total Fe = Fe_2O_3 in Table 3. This procedure yields crystal-chemically valid cation totals and site distributions, and is consistent with the high estimated Fe_2O_3 contents of coexisting alkali amphiboles. Total Fe has been used to construct the classification diagram in Figure 6a; on this basis, the metasomatic mica compositions from the blue sills and remobilized lenses plot as Al-deficient fluorphlogopite and biotite that in most cases require Fe^{3+} to completely fill the T-site, *i.e.*, they trend toward the "tetraferriphlogopite" end-member (Fig. 6a). The mica is Al- and Ti-poor and is similar in composition to mica in kimberlites and ultrabasic (or ultramafic) lamprophyres (Rock 1990; Fig. 6b). Fluorine contents vary from 1.5 to 4.5 wt% (Fig. 6c); the higher levels are significantly greater than normally encountered in primary mica from ultrabasic lamprophyres (Rock 1990).

The mica that rims primary phenocrysts from the dark brown sills and that from fenitized basement granite consist of nondistinctive biotite with a low F content (Fig. 6). Mica phenocrysts from the dark brown sills plot as high-Ti, low-F biotite on Figures 6a–c; they are characterized by higher Ba and Cr contents than the metasomatic mica compositions, although these abundances are lower than found for phenocrystic mica from most ultrabasic lamprophyres and kimberlites (Rock 1990). The mica phenocrysts do not yield crystal-chemically valid structural formulae if recalculated using total Fe = Fe_2O_3, suggesting they have relatively low Fe^{3+}/Fe^{2+} values.

Apatite

The ultrabasic sills, remobilized lenses and fenites contain mostly zoned crystals of fluorapatite, with F contents of ~3–4 wt%. Sr and the *LREE* show variable abundances, with ranges from ~0.5 to 2 wt% for SrO and ~0.1 to 0.5 wt% for Ce_2O_3. Cathodoluminescence (CL) studies of the apatite in the sills and remobilized lenses reveals complex patterns of zonation attributable to variations in concentration of CL activator ions (*e.g.*, Eu^{2+}, Eu^{3+}, Sm^{3+}, Dy^{3+} and Tb^{3+}) incorporated during growth of the zones (Mariano 1989). The pattern of zonation is generally consistent within any particular sample, although it varies between different layers in the composite sills. Zonation textures and the nature of inclusions suggest that most crystals grew in successive stages, from waves of metasomatic fluid

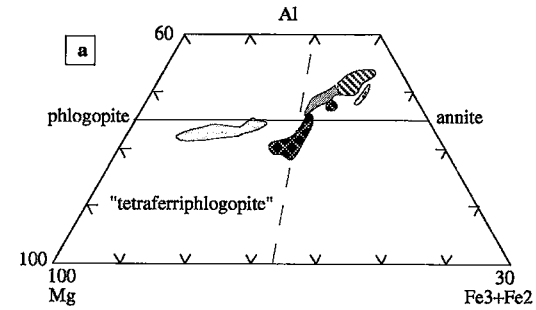

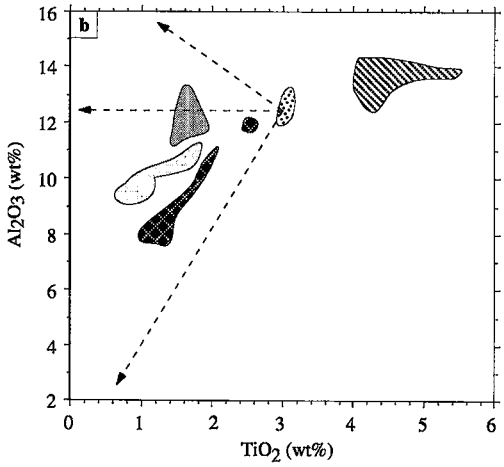

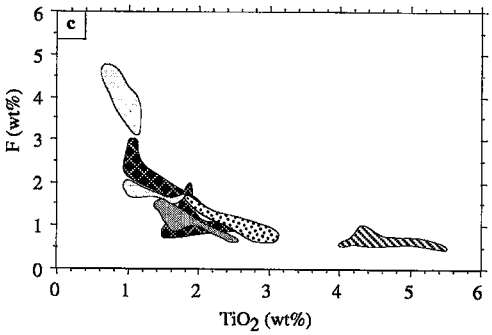

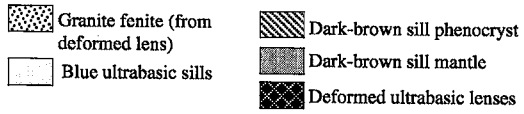

FIG. 6. Compositional variation of mica from the Lyons River ultrabasic sills, remobilized lenses and fenites in terms of a) Al:Mg:(Fe^{3+} + Fe^{2+}), b) Al_2O_3 *versus* TiO_2, a plot showing a comparison to evolutionary trends in mica from kimberlite, as described by Mitchell (1989), and c) F *versus* TiO_2.

with different trace-element contents.

Figure 7 shows a typical aggregate of zoned apatite crystals from a carbonate-rich layer of a composite blue sill. Room-temperature CL spectra are shown for the three principal zones, and the mean compositions of the zones are given in Table 4. The concentration of Sr increases consistently toward the margin of the grain, together with a more erratic increase in Y, Ce and Nd. The core of the aggregate, which shows dark purple luminescence under CL, comprises euhedral grains with numerous silicate inclusions. The core is overgrown successively by an inner rim with pale to dark violet luminescence, and an outer rim of pink luminescence (Fig. 7). Inclusions of sodic pyroxene and phlogopite may occur on zone boundaries. The CL spectra in Figure 7 show that the transition from purple to dark violet zones is due to greater relative importance of heavy rare-earth and Eu^{2+} activators in the inner zones (which emit in the blue-violet part of the spectrum) compared to the *LREE* activators such as Sm, which have a yellow-orange CL emission. This CL pattern of zonation is consistent with decreasing La/Y ratios from core to rim, as revealed by a microprobe traverse (Table 4).

Carbonate

Ferroan dolomite and ferroan magnesite are the dominant carbonates present in the blue sills;

TABLE 4. MEAN COMPOSITION OF ZONES IN APATITE FROM SAMPLE P17138

SAMPLE	P17138	std	P17138	std	P17138	std	P17138	std	P17138	std
CL colour	purple	n=7	purple	n=17	violet	n=30	deep violet	n=5	pink	n=7
Na_2O wt%	0.12	0.02	0.09	0.01	0.17	0.02	0.18	0.02	0.20	0.02
SiO_2	0.10	0.07	0.29	0.09	0.06	0.02	0.07	0.01	0.06	0.02
P_2O_5	41.06	0.48	40.67	0.53	40.01	0.28	39.75	0.23	39.71	0.60
CaO	55.53	0.49	55.55	0.61	55.24	0.41	55.00	0.65	55.17	0.37
FeO	0.05	<0.01	0.07	0.03	0.06	0.01	0.05	<0.01	0.05	<0.01
SrO	0.45	0.04	0.56	0.08	0.67	0.05	0.87	0.06	0.88	0.03
Y_2O_3	0.08	0.01	0.08	<0.01	0.11	0.03	0.19	0.05	0.14	0.05
BaO	0.07	0.03	0.05	<0.01	0.06	0.02	0.05	<0.01	0.06	0.01
La_2O_3	0.13	0.04	0.09	0.03	0.11	0.03	0.07	0.01	0.13	0.04
Ce_2O_3	0.22	0.05	0.19	0.07	0.38	0.07	0.37	0.02	0.34	0.07
Nd_2O_3	0.12	<0.01	0.13	0.02	0.15	0.03	0.20	0.02	0.17	0.03
ThO_2	0.06	0.01	0.05	0.01	0.06	0.02	0.06	0.01	0.06	0.02
UO_2	0.05	0.01	0.07	0.03	0.08	0.05	0.05	<0.01	0.06	0.02
F	3.43	0.01	3.38	0.11	3.47	0.04	3.45	0.03	3.43	0.04
O = F	1.44		1.42		1.46		1.45		1.44	
Total	100.03		99.85		99.17		98.91		99.02	
wt% oxide, total REE+Sr	0.55		0.49		0.75		0.83		0.78	
O = 25										
Na	0.0394		0.0296		0.0567		0.0603		0.0669	
Ca	10.0638		10.1030		10.1735		10.1769		10.1994	
Fe	0.0071		0.0099		0.0086		0.0072		0.0072	
Sr	0.0441		0.0551		0.0668		0.0871		0.0880	
Y	0.0072		0.0072		0.0101		0.0175		0.0129	
Ba	0.0707		0.0507		0.0616		0.0516		0.0618	
La	0.0081		0.0056		0.0070		0.0045		0.0083	
Ce	0.0136		0.0118		0.0239		0.0234		0.0215	
Nd	0.0072		0.0079		0.0092		0.0123		0.0105	
Th	0.0023		0.0019		0.0023		0.0024		0.0024	
U	0.0019		0.0026		0.0031		0.0019		0.0023	
Total	10.2654		10.2855		10.4227		10.4450		10.4811	
P	5.8793		5.8440		5.8218		5.8111		5.8002	
Si	0.0169		0.0492		0.0103		0.0121		0.0104	
Total	5.8962		5.8932		5.8321		5.8232		5.8105	
Cation Total	16.1616		16.1787		16.2548		16.2682		16.2916	
F	1.8350		1.8146		1.8865		1.8844		1.8718	
La/Y	1.1		0.8		0.7		0.3		0.6	

NB: below limit of detection: SO_3 ≤0.05, Al_2O_3 ≤0.05, Pr_2O_3 ≤0.2, $Sm2O3$ ≤0.15, Gd_2O_3 ≤ 0.15, MgO ≤ 0.05, MnO ≤0.05, K_2O ≤0.05, Cl ≤0.05 wt%.

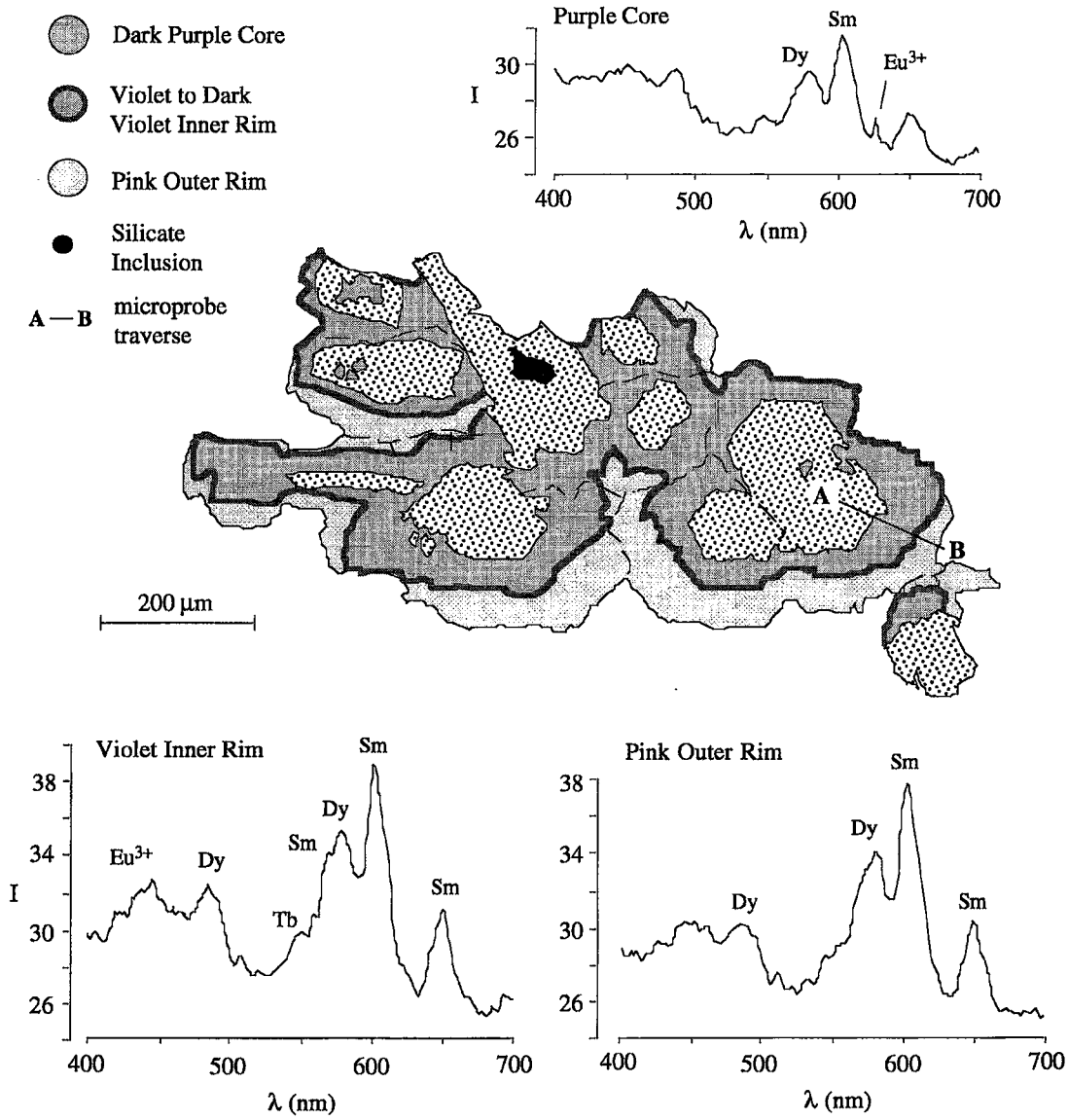

FIG. 7. Cathodoluminescence zonation in, and room-temperature CL spectra for, apatite from sample P17138, a blue composite sill. Average chemical composition of the zones along the traverse A–B is given in Table 4.

magnesite, calcic dolomite and calcite are only rarely encountered. The Mg–Fe-rich compositions of these phases are consistent with textural observations indicating that they may have replaced former ferromagnesian silicates such as olivine. Dark brown sills contain dominantly magnesian calcite and calcic dolomite, and the carbonate in the deformed lenses is calcic dolomite. The grains of ferroan magnesite in the blue sills contains Ca levels below the limit of detection, suggesting that they crystallized below 250°C (Fig. 8). They cannot, therefore, have formed in equilibrium with the ferroan dolomite, which has solid-solution limits indicating a temperature of crystallization of ~450 – 550°C (Fig. 8). The carbonate compositions in the dark brown sills are generally consistent with cocrystallization of magnesian calcite and dolomite at ~500°C. The compositions of the calcic dolomite core from the deformed lenses imply crystallization temperatures above 550°C (Fig. 8).

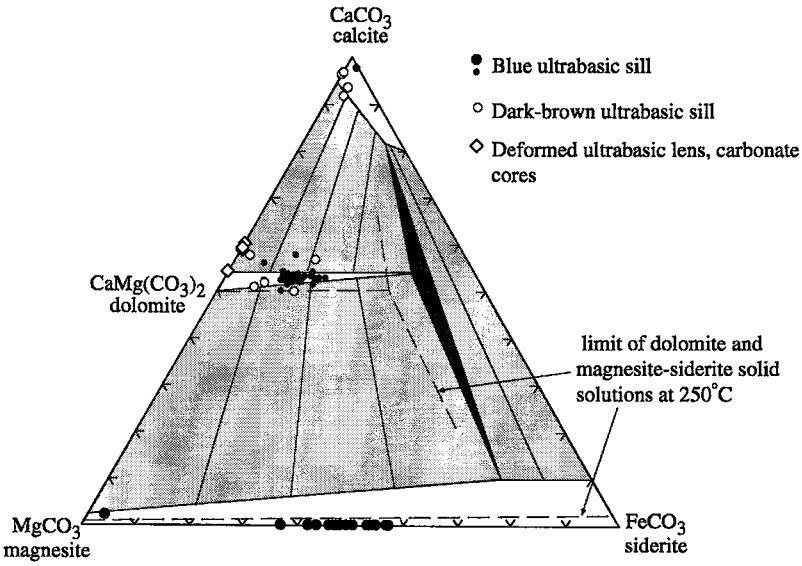

FIG. 8. Composition of carbonate from the Lyons River sills and lenses, plotted on a phase diagram for the carbonate system at 550°C. After Anovitz & Essene (1987).

CL studies indicate that the carbonates in all the rock types are zoned, and in many cases this zoning is complex. In the deformed lenses, uneven cores in dolomite are irregularly replaced and rimmed by a more ferroan dolomite having dull red-brown luminescence. The ferroan dolomite is in turn rimmed by finely zoned dolomite with yellow-orange luminescence. The final carbonate is a weakly luminescent ferroan dolomite that infills cavities and interstices, rims amphibole crystals, and forms fine veinlets.

BULK-ROCK GEOCHEMISTRY

Major and trace elements

Five samples of least-altered blue ultrabasic sills, one of green sill, and four of deformed lens material were analyzed for a full range of major and trace elements. In view of the textural similarities between the blue sills and the Benfontein carbonate-rich kimberlite sills from South Africa, representative samples from the Benfontein middle sills also were analyzed, as complete compositional information is not available in the literature. The Benfontein sill samples analyzed were JJG2243, a carbonate-rich kimberlite with prominent carbonate laths, K18/256, a carbonate-rich kimberlite with "injection layering" texture, K18/310, a carbonate-dominant aphanitic kimberlite with abundant carbonate laths, and JJG2250, a carbonate-rich kimberlite with evidence of settling of olivine. All the samples are from the middle sill and were selected because their lack of weathering.

All the blue sill samples are ultrabasic, low-silica compositions (19–25% SiO_2). They have remarkably low Al contents (1.3–2.6% Al_2O_3), are non-potassic (atomic K/Na <1), and have FeO_t/MgO values that range from ~0.6 to >1.0, suggesting that both relatively primitive and more evolved compositions are present. However, the relatively high Ni (~200–500 ppm) and Cr (~400 to 600 ppm) contents of the sills argue against significant fractionation of olivine, implying that Fe could have been added during fenitization. The overall composition of the rocks resembles that of some types of ultrabasic lamprophyre, such as aillikite (Rock 1990), and various examples of carbonate-rich kimberlite, such as the Benfontein sills and the Igwisi Hills lavas in Tanzania (Dawson & Hawthorne 1973, Taylor *et al.* 1994, Dawson 1994; see Table 5). They are strongly enriched in incompatible elements such as Sr, Ba and the *LREE* (Ce ~300–500 times chondritic abundance) and have steep *REE* patterns (chondrite-normalized La/Yb ≈30–70) similar to many alkaline ultrabasic rocks (Rock 1990).

Despite complete replacement of the primary minerals in the sills, these rocks seem to have retained chemical features characteristic of the primary rock. This can be illustrated in terms of various ratios of compatible and incompatible elements that are usually not strongly suspectible to alteration-related change (Taylor *et al.* 1994). Thus compared to the Benfontein sills, the blue sills have closely similar Ni/MgO (~25–30), Sc/Al_2O_3 (~9), Nb/La (~0.9), Zr/Hf (~40–50), Nb/Zr (~0.4–0.5) and Ce/Sr (~0.2–0.4) values. These values are also similar to those in aillikite, but differ significantly from most examples of non-micaceous kimberlite (see Taylor *et al.* 1994).

TABLE 5. MAJOR- AND TRACE-ELEMENT CHEMISTRY OF THE LYONS RIVER ULTRABASIC SILLS AND DEFORMED LENSES

	ULTRABASIC SILLS						DEFORMED LENSES				BENFONTEIN SILLS			
TYPE	blue	blue	blue	blue	blue	green								
SAMPLE	P01019	P16852	P17119	P17120	P17122	P17128	P17140	P17141	P01089	P01060	JJG2243	JJG2250	K18/256	K18/310
SiO_2	23.90	24.72	19.28	24.85	24.43	7.78	24.32	19.27	20.21	16.70	23.46	27.63	24.23	11.93
TiO_2	3.89	2.80	3.25	3.64	2.21	1.24	3.41	2.37	1.27	3.20	2.50	2.03	4.78	5.92
Al_2O_3	2.40	1.29	1.53	2.60	2.54	0.57	2.95	1.04	1.92	1.26	2.25	1.73	3.12	5.82
$Fe_2O_3^t$	15.89	10.79	15.91	14.68	12.13	13.65	13.06	8.91	15.15	10.18	11.94	11.65	18.14	17.79
MnO	0.24	0.22	0.20	0.21	0.23	0.27	0.18	0.18	0.60	0.21	0.23	0.22	0.30	0.33
MgO	13.02	14.50	13.25	8.86	9.71	8.70	10.22	15.51	14.70	17.28	25.15	30.54	28.22	13.62
CaO	12.69	17.28	14.61	15.42	17.97	28.56	15.37	18.25	16.62	18.02	16.31	12.60	9.14	22.07
Na_2O	2.14	1.97	2.47	3.58	2.70	1.51	2.97	2.19	0.57	1.39	0.45	0.40	0.21	0.66
K_2O	2.41	1.13	1.53	2.33	2.26	0.41	2.94	2.02	2.76	2.30	0.14	0.20	0.09	0.29
P_2O_5	0.74	0.51	1.74	1.61	2.62	2.81	0.37	0.12	0.37	0.01	3.41	2.47	1.22	3.48
F	0.54	0.48	0.40	0.30	0.44	0.33	0.07	0.30	1.00	0.82	na	0.23	0.13	na
LOI	22.21	24.56	25.66	21.09	22.72	33.97	23.77	28.41	25.31	28.52	13.18	9.82	10.40	16.66
O=F	0.23	0.20	0.17	0.13	0.19	0.14	0.03	0.13	0.42	0.35	-	0.10	0.06	-
TOTAL	99.85	99.89	99.66	99.05	99.77	99.66	99.80	98.44	100.06	99.55	99.02	99.63	99.93	98.57
Sc	21.7	12.2	13.7	21.3	24.5	21.9	18.8	8.1	59.7	21.9	19.1	17.1	31.4	33.2
V	276	234	185	254	226	248	243	119	197	356	174	150	220	337
Cr	411	390	468	564	419	70	650	447	520	462	862	947	1740	527
Ni	477	419	326	326	186	27	323	615	220	236	598	853	653	91
Cu	26	79	161	170	158	27	126	317	33	52	109	80	81	96
Zn	172	93	112	86	75	92	103	292	175	105	87	79	121	141
Rb	98	147	44	68	93	21	101	38	291	174	9	25	11	21
Sr	939	843	1237	1198	907	2423	1293	413	275	186	1488	1379	715	2794
Y	29	19.5	14	31	184	173	5	bld	bld	bld	28	20	16	44
Zr	255	235	325	478	468	655	313	182	139	654	532	362	711	1039
Nb	156	94	94	166	141	339	104	103	263	602	235	164	286	515
Ba	1601	494	137	3788	277	404	886	9400	623	3148	2365	1526	1271	5821
Hf	8.5	5.6	7.1	11.6	10.6	11.0	8.8	5.3	5.4	11.4	10.9	7.3	16.0	24.5
La	177	118	122	142	142	224	143	143	788	7.24	252	161	212	484
Ce	371	248	266	296	299	471	302	261	1618	21.8	527	376	497	1193
Nd	152	102	101	113	142	210	107	72.6	545	14.9	219	156	230	513
Sm	21.5	15.4	14.1	17.4	29.3	36.3	12.7	8.1	48.2	2.7	33.1	24.0	32.5	73.4
Eu	4.63	3.80	2.90	4.09	8.77	11.00	2.37	0.96	8.33	0.52	8.20	5.66	7.34	17.70
Tb	1.47	1.36	1.10	1.65	4.11	4.95	0.65	0.42	1.37	0.23	2.00	1.56	1.96	4.17
Dy	na	na	5.72	8.82	na	na	na	na	4.73	1.20	na	na	na	na
Ho	1.41	1.29	1.05	1.76	4.89	5.93	0.56	0.43	0.67	0.20	1.16	1.11	1.11	2.52
Yb	3.17	1.46	1.97	3.64	8.29	10.86	0.69	0.70	0.71	0.29	1.42	1.12	1.12	2.66
Lu	0.46	0.18	0.22	0.52	0.97	1.44	0.09	0.09	0.09	0.03	0.18	0.15	0.15	0.32
Ta	9.4	7.3	13.3	9.8	9.6	30.3	9.4	8.8	6.9	25.0	28.9	13.6	28.9	48.1
Pb	9	20	14	13	18	32	21	24	47	13	27	13	27	31
Th	30.7	17.6	21.4	43.6	47.9	150	31.9	67.5	109	5.3	33.1	25.3	44.3	100
U	6	5	3	bld	4	29	7	6	7	bld	10	7	9	18
wt ratios:														
P_2O_5/Ce	20	21	65	54	87	60	12	5	2	6	65	66	25	29
Nb/Zr	0.61	0.40	0.29	0.35	0.30	0.52	0.33	0.57	1.89	0.92	0.44	0.45	0.40	0.50
Zr/Hf	30	42	46	41	44	60	36	34	26	57	49	50	44	42
Nb/La	0.9	0.8	0.8	1.2	1.0	1.5	0.7	0.7	0.3	83.1	0.9	0.9	1.3	1.1
Ce/Sr	0.39	0.29	0.22	0.25	0.33	0.19	0.23	0.63	5.88	0.12	0.35	0.27	0.70	0.43
Ni/MgO	37	29	25	37	19	3	32	40	15	14	24	28	23	7
Sc/Al_2O_3	9.0	9.5	9.0	8.2	9.6	38.4	6.3	7.7	31.1	17.4	8.5	9.9	10.1	5.7
atomic ratios:														
Na+K/Al	2.6	3.5	3.7	3.2	2.7	5.1	2.7	5.6	2.0	3.8	0.4	0.5	0.1	0.2
K/Na	0.7	0.4	0.4	0.4	0.6	0.2	0.7	0.6	3.2	1.1	0.2	0.3	0.3	0.3

Concentration of major elements, reported as oxides except for fluorine, are expressed in wt.%; concentration of trace elements expressed in ppm. na: not analyzed. $Fe_2O_3^t$: total iron. Detection limits: SiO_2, Al_2O_3, Na_2O: 0.05%; TiO_2, Fe_2O_3, MnO, MgO, CaO, K_2O, LOI: 0.01%; P_2O_5 0.005%; Ba 10 ppm; V, Cr, Ni, Zn, Rb, Sr, Y, Zr, Pb: 5 ppm; Cu: 4 ppm, Nb, Mo, U: 3 ppm; Nd: 2 ppm; Ce, Dy: 1.0 ppm; Tb: 0.5 ppm. The amount of Au is below the limit of detection (5 ppb) in all cases. Samples of the Benfontein sill were taken from the University of Cape Town collection.

Many of these similarities are evident on a primitive-mantle-normalized abundance diagram (Fig. 9), although the Lyons River sills are notably enriched in Rb, K and F, suggesting that these elements, together with Na, have been added during fenitization. The strongly peralkaline character of the sills (atomic [Na + K]/Al ≈2–4), compared to ultrabasic lamprophyres and carbonate-rich kimberlites, suggests that additional alkalis were acquired during fenitization. The F content of the rocks (~0.30–0.54%) is about twice the level of F abundance in the Benfontein sills, suggesting that this element also was added during fenitization.

The green sill is a non-primitive rock (FeO_t/MgO 1.4, Ni 27 ppm) with carbonatitic chemistry (*e.g.*, low Al and high Ca) that is consistent with its mineralogical composition. The Zr/Hf ratio of the rock is high (~60) compared to the range for most mantle-derived magmas (Zr/Hf ~30–40; see Dupuy *et al.* 1992). Fractionation of Zr from Hf does not occur during normal igneous differentiation (*i.e.*, crystal fractionation of mafic silicate phases), but elevated Zr/Hf can be generated by processes involving carbonate liquids such as carbonate–silicate liquid immiscibility (Dupuy *et al.* 1992). The high Zr/Hf ratio of the green sill suggests that it was probably not simply a residuum derived by olivine fractionation of the blue sills. This view is supported by an example of an olivine-fractionated Benfontein carbonate-rich kimberlite composition (K18/310, Table 3) which bears little compositional resemblance to the green sill (*cf.* high levels of TiO_2 and Al_2O_3 of the former).

The deformed lenses have major-element compo-

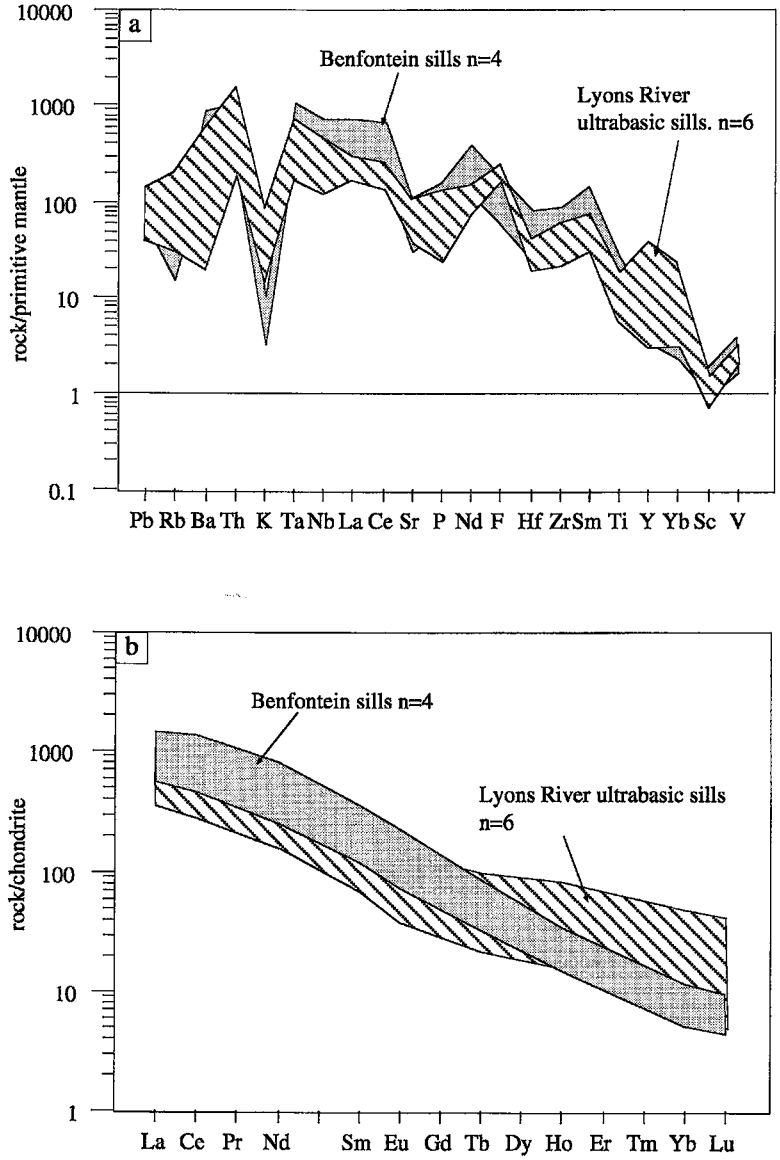

FIG. 9. a) Primitive-mantle-normalized (after Sun & McDonough 1989) incompatible trace elements in the Lyons River ultrabasic sills, compared with the Benfontein sills. b) Chondrite-normalized (after Nakamura 1974) *REE* in the Lyons River ultrabasic sills, compared with the Benfontein sills.

sitions that are similar to those of the blue sills, but in terms of their minor and trace elements, they are highly variable. Some samples show a strong enrichment in Sr, *REE*, Ba, Sc, Rb, and Nb, whereas other samples show a marked depletion. As with the blue sills, they all have peralkaline chemistry, but levels of P and F are significantly lower than in the sills, suggesting that these elements have been mobile.

Stable isotope chemistry

Ferroan dolomite and ferroan magnesite from two samples of blue sills were extracted from the matrix and from the olivine pseudomorphs. The carbonates have an undisturbed $\delta^{13}C$ (Table 6) close to mantle values (–5 to –6‰), but $\delta^{18}O$ values have been shifted upward from the "mantle box" probably due to post-

TABLE 6. STABLE ISOTOPE GEOCHEMISTRY OF PRIMARY TEXTURED SILLS

SAMPLE	LOCATION	δ^{13}C / PDB	δ^{18}O / SMOW
†76718	'olivine' pseudomorph	-5.43	+10.48
†76718	matrix'	-5.24	+10.37
†76716	'matrix'	-5.59	+10.42
#76716	'olivine' pseudomorph	-5.22	+18.36

† = ferroan dolomite
# = ferroan magnesite

emplacement exchange with hydrothermal or meteoric water (*cf.* Kirkley *et al.* 1989). The magnesite sample shows the greatest shift in δ^{18}O. Nevertheless, the δ^{13}C and δ^{18}O values are all within the range reported for carbonates from both the Benfontein sills and the Igwisi Hills lavas (Fig. 10; Kirkley *et al.* 1989, Dawson 1994). It seems remarkable that, despite the strong fenitization overprint affecting the blue sills, the stable isotope compositions of the carbonates are identical to those of compositionally equivalent pristine intrusive and volcanic rocks.

Discussion

Source and nature of alkali metasomatism

The Lyons River metasomatic belt covers an extensive area of country rock and is of a type similar to that found in association with major ijolite-carbonatite or alkaline silicate ring complexes (*e.g.*, nepheline syenite) in other cratonic regions (McKie 1966, LeBas 1977). However, at Gifford Creek, neither of these rock associations has been observed, and there are no exposed alkali silicate rock bodies. Although the most intense fenitization is localized about the Lyons River ultrabasic sills, volumetric and compositional constraints indicate that these bodies are unlikely to have been significant sources of fenitizing fluids over the whole belt. The sills may have been emplaced in a zone of crustal weakness that was also exploited as a pathway for fenitizing fluids. The ultimate source of the fluids may be a larger unexposed igneous body that crystallized at depth during the 1.68 Ga magmatic event. Detailed study of magnetic and gravity anomalies, which are known in the region, would be required to better address such a hypothesis.

The Lyons River fenite belt is mineralogically and chemically zoned in a way that closely resembles some classic fenite localities, such as the Fen complex (Kresten 1988). Thus K-metasomatized granitoid rocks dominate the lower grade (low-temperature) outer zone, whereas metasomatism involving Na ± Fe in addition to K is important in the higher-grade (high-temperature) inner aureole and contact zones. Because the fenitized sills cross-cut K-feldspar veins, there was presumably an earlier low-temperature phase of aureole and vein fenitization, predating sill emplacement, that was later overprinted by the high-grade aureole.

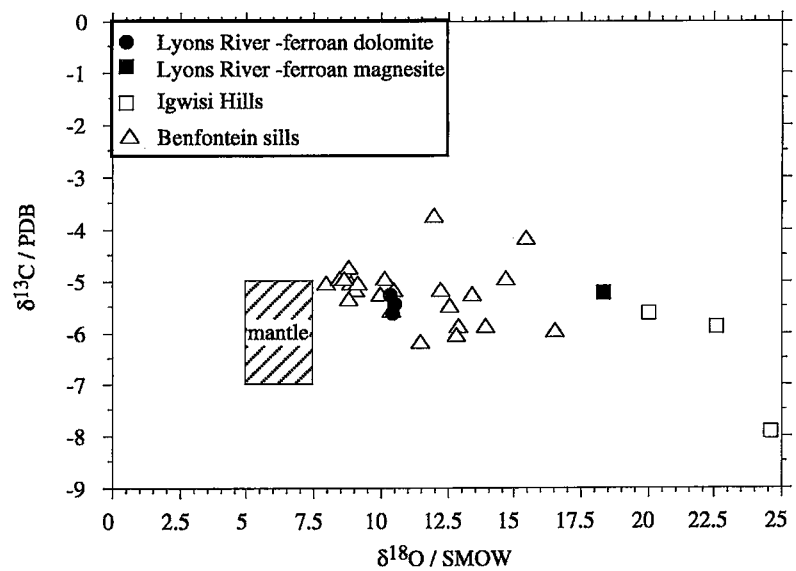

FIG. 10. Stable isotope compositions of the Lyons River ultrabasic sills, compared with samples from the Benfontein calcite kimberlite (Kirkley *et al.* 1989) and Igwisi Hills lavas (Dawson 1994).

Metasomatism of the sills resulted in addition of alkalis (Rb, K, Na), F, and probably Fe, but other minor and trace elements were probably locally mobilized and redistributed within the confines of their host rock. The nature of the metasomatism varied among sill types and between different layers of the composite sills, suggesting that local chemical controls on fluid composition were important. This is evident from local variation in assemblages of the metasomatic minerals, such as variations in minerals replacing olivine, and mutiple zonation involving the *REE*, Sr, *etc.*, in phases such as apatite. The composition retained by dolomite in the sills indicates that high-grade fenitization took place above 450°C, and ~550–650°C is a reasonable estimate for peak temperatures of fenitization based on coexisting carbonates. A notable feature of the fenitized sills is that the matrix and replacement carbonates preserve a stable isotope signature close to that of mantle carbon, as do carbonates from the Benfontein sills. The crustal depth of the system is difficult to judge; the absense of alkaline plutonic rocks indicates that the present exposure represents a relatively high-level section through the system.

Petrographic interpretation of the Lyons River sills

Interpretation of the original igneous mineral assemblage in the blue ultrabasic sills suggests that this rock was composed primarily of olivine macrocrysts and phenocrysts, together with less common mica phenocrysts, set in a groundmass containing perovskite, mica, apatite, titanian magnetite, and carbonate. An igneous classification based on the inferred mineralogy and texture suggests that these rocks have a close affinity to carbonate-rich kimberlites (*e.g.*, Benfontein sills) or ultramafic lamprophyres such as aillikite (Rock 1990). There is no indication that feldspar was a component of the original rock. The younger green sills have a silico-carbonatite composition and consist mainly of carbonate with lesser apatite and sodic pyroxene. They may have formed by carbonate–silicate immiscibility, as suggested by their fractionated Zr/Hf ratios.

Many of the textural features, such as centimeter-scale layering, are very similar to those observed in the Benfontein sills (Dawson & Hawthorne 1973). In the Benfontein sills, carbonate-rich layers are overlain by layers of olivine-rich cumulate that show evidence of gravity settling and load structures at the layer boundaries. These same magmatic features are evident in the Lyons River sills, although the primary minerals have been completely replaced.

Geochemical affinity of the Lyons River sills

It is evident that despite the total metasomatic replacement of the primary igneous minerals, the geochemical signature of the rocks, based on incompatible and compatible elements, is similar to that of the Benfontein sills. The somewhat lower Ni and Cr values, compared to the generally more magnesian Benfontein sills, suggest that some fractionation of olivine and chromian spinel occurred in the Lyons River sills.

Origin of the deformed lenses

The textures of the lenses, the lack of a fenitized halo in the host sediments, and the absence of contact-metamorphic effects suggest that the lenses were emplaced into the overlying sediments in a plastic state at subsolidus temperatures. Experimental studies on the room-temperature deformation of relatively porous carbonate-rich rocks such as chalk (Jones & Leddra 1989), indicate that they readily deform plastically under conditions of moderate deviatoric stress provided a fluid phase is present as a lubricant on grain boundaries. An increase in pore-fluid pressure decreases the stress required to deform a rock in this manner. These factors suggest that the deformed lenses could have originated by plastic remobilization of ultrabasic bodies intruding a fault zone at depth. Extrusion of the bodies into the overlying sediment could have taken place by post-intrusion movement along the fault provided there was sufficient pore-fluid pressure. Alkali metasomatism prior to remobilization may have assisted this process by increasing the porosity of the bodies. The intimate association of Bangemall sediments and ultrabasic rock in some of the lenses suggests that the sediments were largely unconsolidated at the time the lenses were emplaced, *i.e.*, the remobilization immediately postdated initiation of Bangemall sedimentation. Opening of the Bangemall basin, post-1.68 Ga, may have been responsible for reactivation of the fault system along the Lyons River.

There are similarities between this type of remobilization and "rheomorphism", a term that is used to describe rocks with internal form and structure suggesting that a finite amount of plastic flow has taken place (Bates & Jackson 1987). This term is frequently applied to remobilization that is accompanied by partial melting; however, in the case of the Lyons River lenses, partial melting has not been demonstrated.

Summary

1. Fenitized ultrabasic sills of Paleoproterozoic age (1.68 Ga) are associated with a belt of country-rock fenitization along the Lyons River in the Gifford Creek complex, Gascoyne Province, Western Australia. Although the primary minerals of the sills (macrocrysts: olivine ± mica; groundmass: perovskite, mica, apatite, titanian magnetite, and carbonate) have been replaced mainly by alkali amphibole, sodic pyroxene, and rutile during fenitization, original igneous textures,

including centimeter-scale layering and gravity settling of macrocrysts, are well preserved. On both textural and geochemical grounds, the sills resemble some carbonate-rich kimberlites such as the Benfontein sills of South Africa or some ultramafic lamprophyres such as aillikite.

2. The sills are associated with strongly deformed, fenitized ultrabasic lenses that were emplaced plastically into granitoid country-rocks or into the basal unconformity with overlying Bangemall sedimentary rocks, which were unconsolidated at the time. The emplacement postdates the period of fenitization and occurred under subsolidus conditions. The deformed lenses probably represent ultrabasic sills that were plastically remobilized in response to movement on a fault. This would have been promoted by high pore-fluid pressures and a carbonate-rich matrix.

3. Mineralogical and textural zonation of the ~5-km-wide fenite belt, hosted in country-rock migmatites and granites, resembles that of typical fenite complexes, such as at Fen. However, no large bodies of alkaline mafic or felsic rock are known from the area, so that the source of fenitizing fluids is problematic. The fluids may have been derived from an unexposed alkaline intrusive body located either at depth or under more recent cover. The ultrabasic sills may have intruded a zone of crustal weakness that was also exploited as a pathway for fenitizing fluids.

Acknowledgements

The authors thank John Gurney (University of Cape Town) and Melissa Kirkley (BHP, Kelowna) for access to unpublished work and for providing samples of the Benfontein sills. Terry Williams (Natural History Museum) and Brendon Griffin (CMM, University of Western Australia) are thanked for assistance with the electron-microprobe analyses. Pete Woods and Ian Wood (University College London) assisted with the luminoscope observations and X-ray-diffraction determinations, and Paul Wright (Oxford Instruments) kindly offered the use of CL facilities at Oxford Instruments Research Division. WRT acknowledges funding from the Royal Society, London and from the Australian Research Council. JMP acknowledges an APRA–Industry award, the British Council and Geology Key Centre (UWA) for funding, and financial and logistical support from Newcrest Mining Ltd, Perth.

References

Anovitz, L.M. & Essene, E.J. (1987): Phase relations in the system $CaCO_3$–$MgCO_3$–$FeCO_3$. *J. Petrol.* **28**, 389-414.

Bates, R.L. & Jackson, J.A. (1987): *Glossary of Geology* (3rd ed.). American Geological Institute, Alexandria, Virginia.

Chuck, R.G. (1984): The sedimentary and tectonic evolution of the Bangemall Basin, Western Australia, and implications for mineral exploration. *West. Aust. Mining and Petroleum Institute (WAMPRI), Rep.* **6**.

Dawson, J.B. (1994): Quaternary kimberlitic volcanism on the Tanzania Craton. *Contrib. Mineral. Petrol.* **116**, 473-485.

_____ & Hawthorne, J.B. (1973): Magmatic sedimentation and carbonatitic differentiation in kimberlitic sills at Benfontein, South Africa. *J. Geol. Soc. London* **129**, 61-85.

Dupuy, C., Liotard, J.M. & Dostal, J. (1992): Zr/Hf fractionation in intraplate basaltic rocks: carbonate metasomatism in the mantle source. *Geochim. Cosmochim. Acta* **56**, 2417-2423.

Gellatly, D.C. (1975): Yangibana Creek U – Th – REE – base metal prospect, Gascoyne Goldfield, W.A. *Final Rep., Amax Exploration (Australia) Inc.*, 21 p.

Golding, S.D., Groves, D.I., McNaughton, N.J., Barley, M.E. & Rock, N.M.S. (1987): Carbon isotopic composition of carbonates from contrasting alteration styles in supracrustal rocks of the Norseman–Wiluna Belt, Yilgarn Block, Western Australia: their significance to the source of Archean auriferous fluids. *In* Recent Advances in Understanding Precambrian Gold (S.E. Ho & D.I. Groves, eds.). *Univ. of Western Australia, Publ.* **11**, 215-238.

Hawthorne, F.C. (1976): The crystal chemistry of the amphiboles. V. The structure and chemistry of arfvedsonite. *Can. Mineral.* **14**, 346-356.

_____ (1981): Crystal chemistry of the amphiboles. *In* Amphiboles and Other Hydrous Pyriboles (D. Veblen, ed.). *Rev. Mineral.* **9A**, 1-102.

Jones, M.E. & Leddra, M.J. (1989): Compaction and flow of porous rocks at depth. *In* Rock at Great Depth (V. Maury & D. Fourmaintraux, eds.). Balkema, Rotterdam, The Netherlands (891-898).

Kirkley, M.B., Smith, H.S. & Gurney, J.J. (1989): Kimberlite carbonates – a carbon and oxygen stable isotope study. *In* Kimberlites and Related Rocks. 4th Int. Kimberlite Conf. (J. Ross, ed.). *Geol. Soc. Aust., Spec. Publ.* **14**, 264-281.

Kresten, P. (1988): The chemistry of fenitisation: examples from Fen, Norway. *Chem. Geol.* **68**, 329-349.

Le Bas, M.J. (1977): *Carbonatite–Nephelinite Volcanism.* Wiley, New York, N.Y.

Mariano, A.N. (1989): Cathodoluminescence emission spectra of rare earth element activators in minerals. *In* Geochemistry and Mineralogy of Rare Earth Elements (B.R. Lipin & G.A. McKay, eds.). *Rev. Mineral.* **21**, 339-348.

McKie, D. (1966): Fenitization. *In* Carbonatites (O.F. Tuttle & J. Gittins, eds.). Wiley, London, U.K. (261-294).

MIAN, I. & LE BAS, M.J. (1986): Sodic amhiboles in fenites from the Loe Shilman carbonatite complex, NW Pakistan. *Mineral. Mag.* **50**, 187-197.

MITCHELL, R.H. (1989): Aspects of the petrology of kimberlites and lamproites: some definitions and distinctions. *In* Kimberlites and Related Rocks; 4th Int. Kimberlite Conf. (J. Ross, ed.). *Geol. Soc. Aust., Spec. Publ.* **14**, 7-45.

MUHLING, P.C. & BRAKEL, A.T. (1985): Geology of the Bangemall Group – the evolution of an intracratonic Proterozoic basin. *West. Aust. Geol. Surv., Bull.* **128**.

NAKAMURA, N. (1974): Determination of REE, Ba, Fe, Mg, Na, and K in carbonaceous and ordinary chondrites. *Geochim. Cosmochim. Acta* **38**, 757-775.

NEWCREST MINING LTD. (1989): Gifford Creek Annual Report 1989. *West. Aust. Dep. Mines and Energy, Open-File Rep.* **A36888**.

ROCK, N.S. (1990): *Lamprophyres*. Blackie & Son, Glasgow, U.K.

SIEMIATKOWSKA, K.M. & MARTIN, R.F. (1975): Fenitization of Mississagi Quartzite, Sudbury area, Ontario. *Geol. Soc. Am., Bull.* **86**, 1109-1122.

SUN, S.-S. & MCDONOUGH, W.F. (1989): Chemical and isotopic systematics of ocean basalts; implications for mantle compositions and processes. *In* Magmatism in the Ocean Basins (A.D. Saunders & M.J. Norry, eds.). *Geol. Soc., Spec. Publ.* **42**, 313-345.

TAYLOR, W.R., TOMPKINS, L.A. & HAGGERTY, S.E. (1994): Comparative geochemistry of West African kimberlites: evidence for a micaceous kimberlite endmember of sublithospheric origin. *Geochim. Cosmochim. Acta* **58**, 4017-4037.

WARE, N.G. (1980): Computer programs and calibration with the PIBS technique for quantitative electron probe analysis using a lithium-drifted silicon detector. *Comput. Geosci.* **7**, 167-184.

WILLIAMS, S. (1986): Geology of the Gascoyne Province. *West. Aust. Geol. Surv., Rep.* **15**.

Received September 27, 1994, revised manuscript accepted August 4, 1995.